



meso-C₆F₅ substituted BODIPYs with distinctive spectroscopic properties and their application for bioimaging in living cells



Junchao Xu^a, Leiming Zhu^a, Qiusheng Wang^a, Lintao Zeng^{a,b,*}, Xichao Hu^b, Boqiao Fu^b, Zhe Sun^{a,*}

^aTianjin Key Laboratory of Organic Solar Cells and Photochemical Conversion, School of Chemistry & Chemical Engineering, Tianjin University of Technology, Tianjin 300384, PR China

^bDepartment of Chemistry and Material Sciences, Hubei Engineering University, Hubei, Xiaogan 432000, PR China

ARTICLE INFO

Article history:

Received 27 January 2014

Received in revised form 5 June 2014

Accepted 12 June 2014

Available online 17 June 2014

Keywords:

BODIPY

Spectroscopic

Bio-imaging

Near infrared region (NIR)

Ethylene glycol

ABSTRACT

A series of *meso*-C₆F₅ BODIPYs have been successfully synthesized and characterized. Some of them displayed excellent spectroscopic properties, such as relatively large Stokes shift, high fluorescence quantum yield, far-red or near infrared region (NIR) emission, and good photostability. In particular, the dye functionalized with oligo(ethylene glycol) ether-phenyl groups at the 3,5-position of BODIPY core became water-soluble and its emission located in the NIR region with large Stokes shift. Time-dependent density functional theory calculations were conducted to understand the structure–optical properties relationship. Furthermore, cell staining tests demonstrated that the *meso*-C₆F₅ BODIPY derivative with oligo(ethylene glycol) ether-phenyl group was membrane permeable and selectively stained cytosol in living cells.

© 2014 Elsevier Ltd. All rights reserved.

1. Introduction

4,4-Difluoro-4-bora-3a,4a-diaza-s-indacene, also known as BODIPY, has gained recognition as one of the most versatile fluorophores over the past two decades.^{1–4} This dye family display superior photophysical properties over other dyes, such as large molar absorption coefficient, high fluorescence quantum yields, good photochemical, and chemical stabilities. Therefore, they have diverse applications including biological imaging and labeling,^{5–7} sensors,^{8–11} photodynamic therapy reagent,^{12,13} dye-sensitized solar cells (DSSC),^{14–16} and light-emitting materials for electroluminescent devices.^{17–19}

For bio-imaging application, a fluorescent dye with far-red or NIR emission, large Stokes shift, and water-solubility is highly desired, because it can minimize auto-fluorescence background and increase penetration of excitation and emission light through tissues.²⁰ BODIPY core usually exhibits visible absorption and emission (470–530 nm) with small Stokes shift (~10 nm), which is not ideal for bioimaging in living animals.²¹ To push the emission spectra to red and even NIR region, a variety of strategies have been used: 1) extension of π -conjugation by fusing rigid ring to the

pyrrole unit (e.g., replacing pyrrole with isoindole),^{22–24} 2) substitution of the 3,5-position by styryl groups,^{25–28} and 3) replacement of the 8-carbon atom with nitrogen atom to form aza-BODIPY dyes.^{29–31} By these methods, various BODIPY dyes with emission wavelength ranging from 560 to 820 nm were obtained. Unfortunately, these compounds showed small Stokes shift and poor water solubility.^{1,2} To modulate the spectroscopic properties, intramolecular charge transfer mechanism is often employed, because an donor (D) and an acceptor (A) linked to a π -conjugation (D- π -A) is beneficial for red-shift in the absorption/emission spectra and large Stokes shift.^{12,32,33}

In this study, we combined two strategies: 1) intramolecular charge transfer mechanism and 2) extension of π -conjugation all together to push the absorption and emission spectra to the far-red and even NIR region. Firstly, a pentafluorophenyl group (C₆F₅) with strong electron-withdrawing character was introduced to the *meso*-position of BODIPY core, and then aromatic groups were attached to the 3,5-position of *meso*-C₆F₅ BODIPY by Suzuki Coupling or Knoevenagel condensation, which is inclined to generate a push–pull type structure and extension of the π -conjugation. As a result, the absorption and emission spectra can be pushed to the far-red or NIR region. To improve the water solubility and cell permeability of *meso*-C₆F₅ BODIPY, ethylene glycol ether was linked to the 4-position of phenyl group. The spectroscopic properties of these newly synthesized BODIPYs were investigated. Some of them

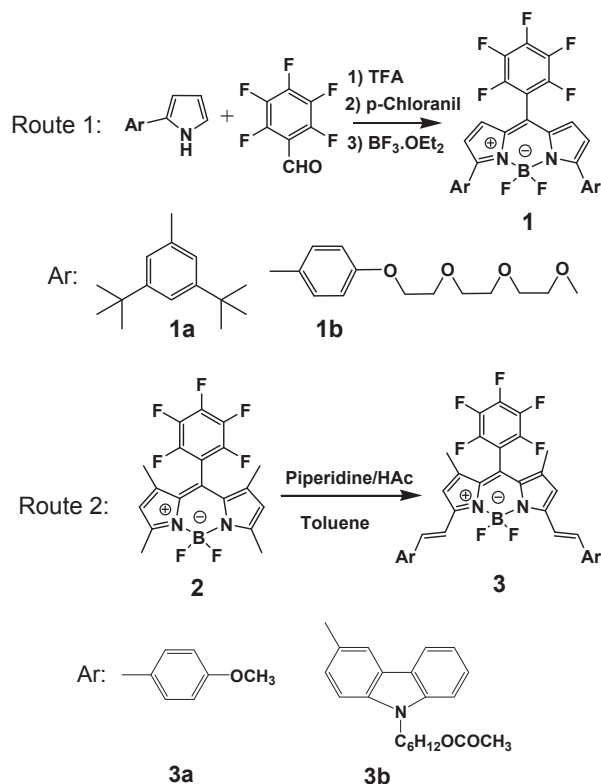
* Corresponding authors. E-mail addresses: 407650531@qq.com, zlt1981@126.com (L. Zeng).

exhibited tunable absorption and emission spectra in the far-red or even NIR region with acceptable fluorescence quantum yields and large Stokes shifts. Time-dependent density functional theory (TD DFT) calculations were conducted to get more insight of their optical properties. Furthermore, cell staining experiments were performed to probe their potentials for bioimaging applications.

2. Results and discussion

2.1. Synthesis

The *meso*-C₆F₅ BODIPYs with 3,5-aryl groups were synthesized in two routes, as were shown in Scheme 1. 1) Pentafluorobenzaldehyde condensed with 2-arylpyrrole in the presence of trifluoroacetic acid (TFA) in dichloromethane (DCM) followed by oxidative dehydrogenation with tetrachloro-*p*-benzoquinone and complexation with BF₃·Et₂O to give the corresponding *meso*-C₆F₅ BODIPYs with 3,5-aryl groups **1a** in 38% and **1b** in 40% yield, respectively. 2) *meso*-C₆F₅ substituted 1,3,5,7-tetramethyl BODIPY **2** was synthesized in the same procedure. Then, **2** condensed with 4-methoxybenzaldehyde/3-carbazolealdehyde in the presence of piperidine and acetic acid to give the desired products in high yields (78%–92%). The yield has been significantly improved compared to ordinary BODIPY derivative.^{34–36} The C₆F₅ group was a strong electron-withdrawing group, which made the methyl groups activated. Consequently, the condensation between 3,5-dimethyl BODIPY and aldehydes were completed in 3 h and afforded the desired products in high yields (78%–92%) even without the aid of Dean–Stark apparatus. This approach was very convenient and effective for construction of double bond by condensation of BODIPY with aldehydes.



Scheme 1. Synthetic routes for *meso*-C₆F₅ BODIPYs.

2.2. Optical properties

Fig. 1 shown the UV–vis–NIR absorption spectra of *meso*-C₆F₅ substituted BODIPYs in dichloromethane, and these photophysical data were listed in Table 1. For the *meso*-C₆F₅ substituted 1,3,5,7-tetramethyl BODIPY (**2**), the maximum absorption peak (λ_{abs}) located at 517 nm ($\epsilon=3.14 \times 10^4 \text{ M}^{-1} \text{ cm}^{-1}$), which exhibited a bathochromic shift of 16 nm in contrast to those of the congeners with phenyl substituents.³⁷ A small bathochromic shift was attributed to inductive effect of the *meso*-C₆F₅ group. **2** also displayed a strong emission band centered at 528 nm (shown in Fig. 2), and its emission spectrum was mirror to its absorption spectrum with a small Stokes shift ($\Delta\nu=478 \text{ cm}^{-1}$), which was similar to ordinary *meso*-aryl BODIPYs. It was noteworthy that the fluorescence quantum yield of **2** was 0.92, which was improved relative to 0.65 for the common *meso*-phenyl BODIPY analog.^{1,37} Such a difference was mainly attributed to the steric effects and an interaction between the fluorine of C₆F₅ group and methyl groups (see Supplementary data, Figs. S16–S20). In this case, the non-radioactive relaxation was blocked and the fluorescence quantum yield was improved.

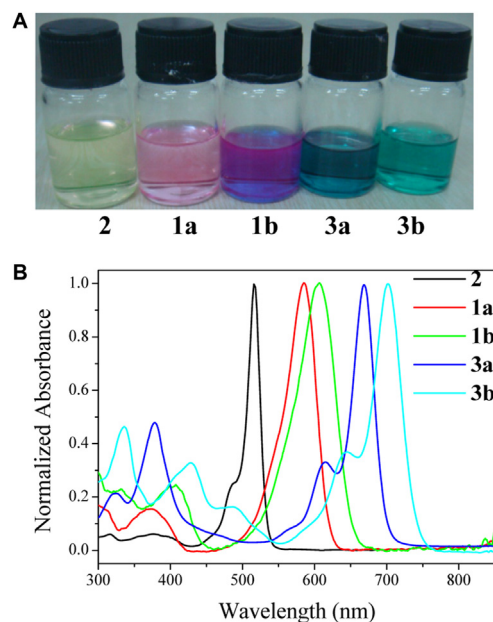


Fig. 1. (A) Images of *meso*-C₆F₅ BODIPYs in DCM; (B) Normalized absorption spectra of *meso*-C₆F₅ BODIPYs in DCM.

By attachment of 3,5-di(*tert*) phenyl groups at the 3,5-positions of *meso*-C₆F₅ BODIPY, a significant bathochromic shift ($\sim 80 \text{ nm}$) in the absorption spectra was observed. The maximum absorption band of **1a** centered at 585 nm ($\epsilon=7.21 \times 10^4 \text{ M}^{-1} \text{ cm}^{-1}$) and the maximum emission band located at 613 nm with a moderate Stokes shift ($\Delta\nu=781 \text{ cm}^{-1}$). Although **1a** exhibited high quantum yield and good solubility in common organic solvents from hexane to methanol, it was completely insoluble in aqueous solution. To improve the water solubility of *meso*-C₆F₅ substituted BODIPY, ethylene glycol ether was introduced to the 4-position of phenyl group. Interestingly, this modification induced a remarkable bathochromic shift in both absorption and emission spectra. As shown in Fig. 3a, **1b** displayed a strong absorption band centered at 607 nm ($\epsilon=4.36 \times 10^4 \text{ M}^{-1} \text{ cm}^{-1}$) and a characteristic emission band at 652 nm with a large Stokes shift ($\Delta\nu=1137 \text{ cm}^{-1}$). In compound **1b**, alkoxy group served as an electron donor (D) while *meso*-C₆F₅

Table 1
The photophysical properties of *meso*-C₆F₅ BODIPYs in DCM

	λ_{abs} (nm)	ϵ (M ⁻¹ cm ⁻¹)	λ_{em} (nm)	Φ	$\Delta\nu$ (cm ⁻¹)
1a	585	7.21×10^4	613	0.61	781
1b	607	4.36×10^4	652	0.40	1137
2	517	3.14×10^4	528	0.92	478
3a	668	2.31×10^4	680	0.08	264
3b	702	4.90×10^4	717	0.003	298

Quantum yields of **1a** and **1b** were determined by using rhodamine B (quantum yield=0.65) as standard in EtOH.³⁸ Quantum yield of **2** was determined by use of fluorescein (fluorescence quantum yield is 0.90 in 0.1 N NaOH) as a standard. For **3a** and **3b**, methylene blue in MeOH ($\Phi=0.03$) was used as standard.

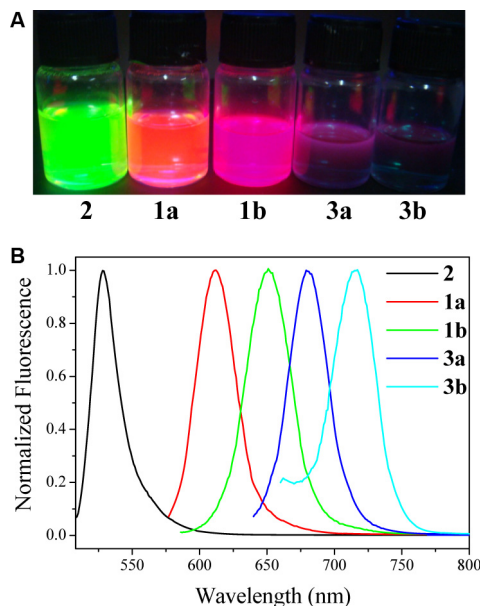


Fig. 2. (A) Fluorescent images of *meso*-C₆F₅ BODIPYs in DCM taken at room temperature under 365 nm UV light; (B) Normalized emission spectra of *meso*-C₆F₅ BODIPYs in DCM.

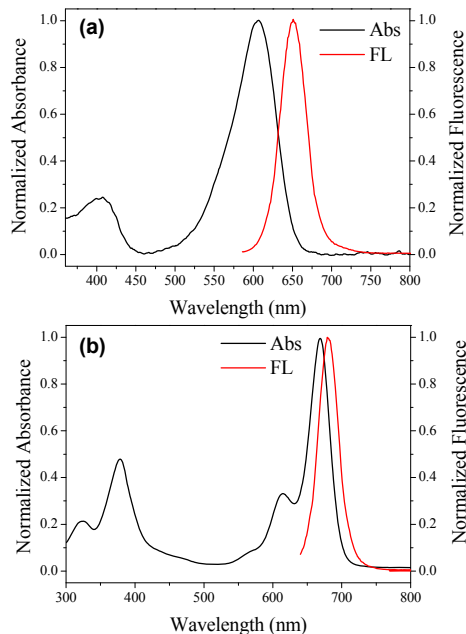


Fig. 3. Normalized absorption and emission spectra of **1b** (a) and **3a** (b) in DCM.

BODIPY was a strong electron acceptor (A). Thus, such a D- π -A structure was benefit for red-shift in the absorption and emission spectra. Thanks to the ethylene glycol ether group, **1b** displayed the far-red region emission and water solubility. The fluorescence quantum yields of **1b** in aqueous solution were also determined, as were shown in Table S1. In aqueous solution containing 10% DMSO, the quantum yield of **1b** was determined as 0.04%, which was favorable for bioimaging.

To further tune the absorption and emission to longer wavelength, 4-methoxybenzylaldehyde/3-carbazolealdehyde condensed with the *meso*-C₆F₅ substituted 1,3,5,7-tetramethyl BODIPY to extend the π -conjugation, resulting in significant red-shifts in both absorption and emission spectra. As shown in Fig. 3b, the maximum absorption band of **3a** centered at 668 nm ($\epsilon=2.31 \times 10^4$ M⁻¹ cm⁻¹) and the maximum emission band located at 680 nm with a small Stokes shift ($\Delta\nu=264$ cm⁻¹). The *meso*-C₆F₅ BODIPY functionalized with 3-carbazolealdehyde displayed a characteristic absorption band centered at 702 nm ($\epsilon=4.90 \times 10^4$ M⁻¹ cm⁻¹) and a weak emission band located at 717 nm. Despite remarkable bathochromic shifts in both absorption and emission spectra, **3a** and **3b** exhibited much weaker fluorescence compared with **1a** or **1b**. *meso*-C₆F₅ group was a strong electron-withdrawing group, whereas 4-methoxyphenyl and 3-carbazolyl groups were typical electron-donating groups. In the excited state, strong intramolecular charge transfer and even electron transfer would happen between *meso*-C₆F₅ BODIPY group and 4-methoxyphenyl/3-carbazolyl groups, resulting in decreased quantum yields. In addition, intersystem crossing would take place due to *meso*-C₆F₅ group, which also led to low quantum yields.

1a, **1b**, and **2** were high emissive in dichloromethane, and their fluorescence quantum yields were significantly improved in comparison to the non-fluorinated *meso*-phenyl BODIPYs analog. As shown in Table 1, the quantum yields of **2**, **1a**, and **1b** in DCM were 0.92, 0.61, and 0.40, respectively. The absorption spectra of **1a** exhibited very weak solvent-dependence, while the absorption spectra of **3a** displayed obvious solvent-dependence (shown in Supplementary data, Fig. S1). In addition, **1a** and **1b** displayed much larger Stokes shifts in contrast to **3a** and **3b**, and these Stokes shifts did not vary much when the solvents were changed from methanol to hexane. This observation implied that the large Stokes shifts were not caused by different permanent dipole moments in the electronic ground and excited state. Aryl groups in **1a** and **1b** could rotate around the C–Ar bonds in the excited state, and the geometry of these compounds could be adjusted, which contributed to a much larger Stokes shift. By contrast, the Aryl groups in **3a** and **3b** were linked to double bonds, which restricted their rotations around the C–Ar bonds in the excited state.

Finally, we examined the photostabilities of these *meso*-C₆F₅ substituted BODIPYs. The fluorescence intensity of representative dyes **1b**, **2**, **3a** in DMF solution and fluorescein in 0.1 M NaOH aqueous solution was measured under continuous irradiation with a 150 W Xe lamp. After exposure to irradiation for 120 min, the fluorescence intensity of fluorescein decreased to 86%, whereas **1a** and **2** remained their fluorescence intensity up to 98%, as were shown in Fig. 4. Therefore, these BODIPYs had excellent photostabilities.

2.3. DFT calculations

To get more insight of the optical properties of this new type of *meso*-C₆F₅ substituted BODIPY dyes, time-dependent DFT calculations were conducted at the B3LYP/6–31G* level of theory for the model compounds.

The calculated frontier molecular orbital profiles and energy levels were shown in Fig. 5. For **1b** and **3a**, the HOMO were delocalized through pyrrole units of BODIPY core to the aryl groups,

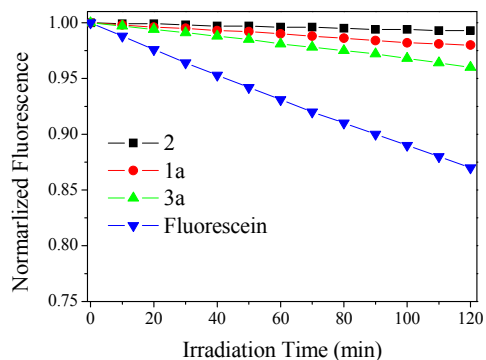


Fig. 4. Changes of fluorescence intensity ($c=5 \mu\text{M}$) under the irradiation of 150 W Xe lamp.

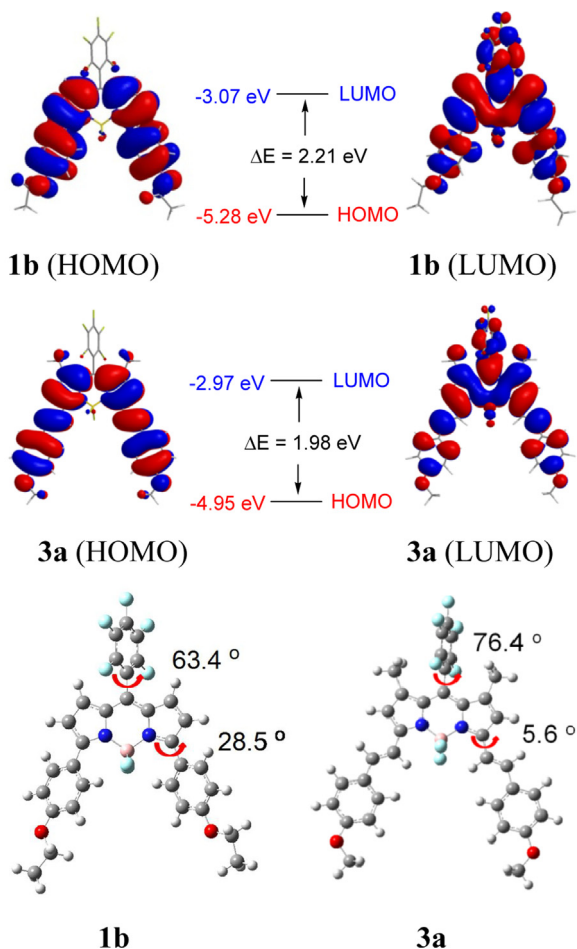


Fig. 5. Calculated frontier molecular orbital profiles, the HOMO/LUMO energy levels and optimized geometries of **1b** and **3a**. To simplify calculation, the ethylene glycol ether group was replaced by ethoxyl group.

while the LUMO mainly located on the BODIPY core and *meso*-C₆F₅ group, implying an intramolecular push–pull character, which was benefit for the bathochromic shift in the absorption spectra. Especially, the LUMO of **3a** mainly located on the *meso*-C₆F₅ group and the BODIPY core with a partial disjoint feature, which also explained the large red shift in the absorption spectra and low fluorescence quantum yield due to strong intramolecular charge transfer. The band gaps of **1b** and **3a** were calculated to be 2.21 eV and 1.98 eV, respectively.

The geometries of *meso*-C₆F₅ substituted BODIPYs have been optimized using time-dependent DFT calculations, as were shown in Fig. 5. The six-member ring of BODIPY core was almost planar and the boron atom was tetrahedral with the two fluorine atoms perpendicular to the BODIPY plane. The optimized geometry of **1b** in the ground state showed a large twist of the *meso*-C₆F₅ group from the BODIPY plan with a torsion angle of 63.4°. Hence, the *meso*-C₆F₅ group just imposed inductive effect on BODIPY core. In the optimized geometry of **1b**, 4-ethoxyphenyl group was slightly out of the BODIPY plane with a torsion angle of 28.5°, and the π -electron was partially delocalized along with BODIPY core, which resulted in red-shift in the absorption and emission spectra. Besides, 4-ethoxyphenyl group might locate at the same plane with BODIPY at the excited state by rotation a certain degree, and then it returned to the ground state, giving rise to a long wavelength emission with a large Stokes shift.³⁹ In the optimized geometry of **3a**, the pentafluorophenyl was nearly perpendicular to the BODIPY plane with an angle of 76.4°, while two styryl groups almost located at the same plane with BODIPY core (a torsion angle of 5.6°). In this case, the π -electrons of 4-methoxyphenyl group were completely delocalized along with BODIPY core. As a result, the absorption and emission spectra of **3a** fell into the near infrared region, as was shown in Fig. 3b.

2.4. Confocal fluorescence imaging

Encouraged by the outstanding feature of **1b**, *epi*-fluorescent microscope was then employed to examine the imaging ability of **1b** in living cells. HeLa cells were co-incubated with **1b** (1.0 μM) and a commercially nucleus-specific staining probe Hoechst (10 μM) for 1 h. By excitation at 638 nm, a clear cell profile with red color was obtained from **1b** (shown in Fig. 6), implying that **1b** could efficiently diffuse into HeLa cells and retained within.^{40,41} According to overlay images of blue fluorescence (Fig. 6b) from Hoechst and red fluorescence from **1b**, it was found that **1b** selectively stained cytosol. Furthermore, by examining the bright-field image, fluorescence image, and overlay image (shown in Fig. 7), we observed that **1b** mainly located in cytosol even at low concentration. **1b** was an amphiphilic compound, thus it met the criteria for a selective cytosol probe in terms of size and amphiphilicity. Therefore, **1b** could be used as a novel probe for selectively staining and bioimaging cytosol.

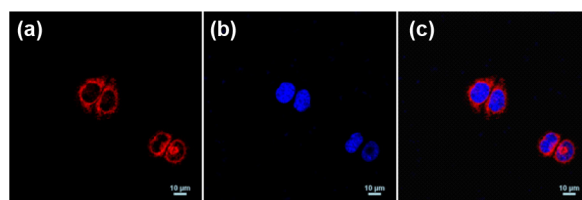


Fig. 6. Confocal fluorescence images of HeLa cells. HeLa cells were co-stained with **1b** (1.0 μM) and Hoechst (10 μM) for 1 h. Fluorescence image was obtained from (a) **1b** at 660 nm ($\lambda_{\text{ex}}=638 \text{ nm}$); (b) Hoechst at 432 nm ($\lambda_{\text{ex}}=405 \text{ nm}$); (c) Merged image of (a) and (b); (60 \times objective lens).

3. Conclusions

In summary, *meso*-C₆F₅ substituted 1,3,5,7-tetramethyl BODIPY was successfully synthesized and characterized. Motivated by its bright fluorescence with small Stokes shift, we have further modified the structure and prepared *meso*-C₆F₅ substituted BODIPYs with extended π -conjugation (**1–3**), which displayed fluorescence emission ranging from 528 to 715 nm. By introduction of oligo(-ethylene glycol) ether substituted phenyl groups at the 3,5-position

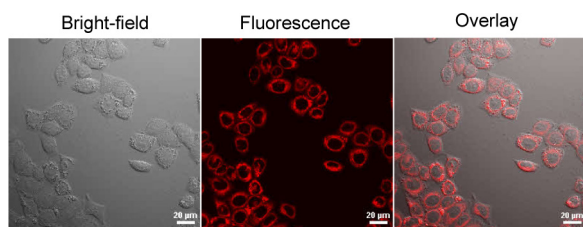


Fig. 7. Confocal fluorescence images of HeLa cells. HeLa cells were incubated with **1b** (2.5 μM) for 0.5 h. Fluorescence image was obtained at 660 nm ($\lambda_{\text{ex}}=638$ nm); 60 \times objective lens; scale bar: 20 μm .

of BODIPY core, it became water-soluble and remained appreciable fluorescence quantum yield with large Stokes shift. The cell staining tests indicated that they were membrane permeable and selectively sustained cytosol in living HeLa cells. All these features made these dyes attractive for bioimaging applications. In addition, our synthetic strategies were very convenient and effective for preparing a series of *meso*-C₆F₅ substituted BODIPY dyes.

4. Experimental section

4.1. Materials

2,3,4,5,6-Pentafluorobenzaldehyde was purchased from TCI corporation. 2,4-dimethyl-pyrrole, tetrachloro-*p*-benzoquinone, Pd(PPh₃)₄ were supplied by Sigma–Aldrich. Pyrrole, BF₃·OEt₂, triethylamine, trifluoroacetic acid, 4-methoxybenzaldehyde, 6-(2-formyl-9*H*-carbazol-9-yl)hexyl acetate, piperidine and acetic acid were supplied by Aladdin-Reagent Corporation. All these compounds were used directly without further purification. The solvents used for UV–vis and fluorescence measurements are of HPLC grade. Fluorescent images were acquired on a Nikon A1 confocal laser-scanning microscope with a 60 objective lens.

4.2. Synthesis

4.2.1. Synthesis of 3,5-bis(3,5-di(*tert*)phenyl)-8-pentafluorophenyl-4,4-difluoro-4-borata-3a,4a-diaza-*s*-indacene (1a**).** 2,3,4,5,6-Pentafluorobenzaldehyde (49 mg, 0.25 mmol) and 2-(3,5-di(*tert*)phenyl)-1*H*-pyrrole (380 mg, 0.52 mmol)⁴² were dissolved in 20 mL of dry DCM in a round bottom flask, and then two drops of trifluoroacetic acid (TFA) were added. The reaction mixture was stirred for 3 h at room temperature in nitrogen. After complete consumption of aldehyde (which was monitored by TLC), tetrachloro-*p*-benzoquinone (63 mg, 0.26 mmol) was added to the reaction mixture. 1 h later, 2 mL of triethylamine and 3 mL of BF₃·OEt₂ were added to the mixture. The resulting mixture was stirred at room temperature for 1 h. When the reaction was completed, the solvent was removed under reduced pressure. The residue was purified by silica gel column chromatography using DCM/hexane (1/5, v/v) as eluent to give compound **1a** as a purple solid (70 mg, 38%). ¹H NMR (300 MHz, CDCl₃): δ 7.76 (s, 4H), 7.52 (s, 2H), 6.76 (d, *J*=4.3 Hz, 2H), 6.65 (d, *J*=4.3 Hz, 2H), 1.39 (s, 36H). ¹³C NMR (125 MHz, CDCl₃): δ 162.0, 150.5, 135.9, 131.6, 128.8, 124.3, 123.7, 122.1, 34.9, 31.4. ¹⁹F NMR (376 MHz, CDCl₃): δ -133.90 (m, 2F), -150.55 (t, 1F), -137.10 (d, 2F), -133.58 (q, 2F). HRMS (EI): [M]⁺=734.3652; calcd for C₄₃H₄₆BF₇N₂: 734.3642.

4.2.2. Synthesis of 3,5-bis(4-(2-(2-(2-methoxyethoxy)ethoxy)ethoxy)phenyl)-8-pentafluorophenyl-4,4-difluoro-4-borata-3a,4a-diaza-*s*-indacene (1b**).** 2,3,4,5,6-Pentafluorobenzaldehyde (98 mg, 0.50 mmol) and 2-[2-(2-methoxyethoxy)ethoxy]ethoxyphenylpyrrole (335 mg, 1.1 mmol) were dissolved in 20 mL of dry

DCM in a round bottom flask, and then two drops of trifluoroacetic acid (TFA) were added. The reaction mixture was stirred for 3 h at room temperature in nitrogen. After complete consumption of aldehyde (which was monitored by TLC), tetrachloro-*p*-benzoquinone (135 mg, 0.55 mmol) was added to the reaction mixture. 1 h later, 4 mL of triethylamine and 6 mL of BF₃·OEt₂ were added to the mixture. The resulting mixture was stirred at room temperature for 1 h. When the reaction was completed, the solvent was removed under reduced pressure. The residue was purified by silica gel column chromatography using DCM/methanol (8/1, v/v) as eluent to give compound **1b** as blue oil (167 mg, 40%). ¹H NMR (400 MHz, CDCl₃): δ 7.90 (d, *J*=8.8 Hz, 4H), 6.98 (d, *J*=8.8 Hz, 4H), 6.70 (d, *J*=4.4 Hz, 2H), 6.65 (d, *J*=4.4 Hz, 2H), 4.19 (t, *J*=5.0 Hz, 4H), 3.88 (t, *J*=5.0 Hz, 4H), 3.75 (q, *J*=5.0 Hz, 4H), 3.70–3.65 (m, 8H), 3.55 (q, *J*=5.0 Hz, 4H), 3.38 (s, 6H). ¹³C NMR (125 MHz, CDCl₃): δ 160.4, 160.0, 139.3, 136.0, 131.3, 128.6, 124.7, 124.0, 123.5, 121.6, 115.9, 114.6, 114.0, 71.9, 70.8, 70.7, 70.6, 69.6, 67.5, 59.0. ¹⁹F NMR (376 MHz, CDCl₃): δ -159.88 (m, 2F), -150.53 (t, 1F), -137.00 (t, 2F), -133.00 (m, 2F). HRMS (EI): [M]⁺=834.2915; calcd for C₄₁H₄₂O₈N₂BF₇: 834.2922.

4.2.3. Synthesis of 1,3,5,7-tetra(methyl)-8-pentafluorophenyl-4,4-difluoro-4-borata-3a,4a-diaza-*s*-indacene (2**).** 2,3,4,5,6-Pentafluorobenzaldehyde (196 mg, 1 mmol) was dissolved in 20 mL of dry DCM in a round bottom flask, and then 2,4-dimethylpyrrole (234 mg, 2.2 mmol) and two drops of trifluoroacetic acid (TFA) were added. The reaction mixture was stirred for 3 h at room temperature in nitrogen. After complete consumption of aldehyde (which was monitored by TLC), tetrachloro-*p*-benzoquinone (270 mg, 1.1 mmol) was added to the reaction mixture. 1 h later, 4 mL of triethylamine and 5 mL of BF₃·OEt₂ were added to the mixture. The resulting mixture was stirred at room temperature for 1 h. When the reaction was completed, the solvent was removed under reduced pressure. The residue was purified by silica gel column chromatography using DCM/hexane (1/6, v/v) to give compound **2** as a golden solid (136 mg, 33%). ¹H NMR (300 MHz, CDCl₃): δ 6.06 (s, 2H), 2.57 (s, 6H), 1.72 (s, 6H). ¹³C NMR (125 MHz, CDCl₃): δ 157.8, 141.5, 131.0, 122.2, 31.6, 29.7. ¹⁹F NMR (376 MHz, CDCl₃): δ -159.52 (m, 2F), -150.53 (t, 1F), -146.14 (q, 2F), -139.25 (q, 2F). HRMS (EI): [M]⁺=414.1141; calcd for C₁₉H₁₄BF₇N₂: 414.1138.

4.2.4. Synthesis of 3,5-bis(4-methoxystyryl)-8-pentafluorophenyl-4,4-difluoro-4-borata-3a,4a-diaza-*s*-indacene (3a**).** Compound **2** (82 mg, 0.2 mmol) and 4-methoxybenzaldehyde (60 mg, 0.44 mmol) were dissolved in 25 mL of toluene in a three-neck round bottom flask. Two drops of piperidine were added to the reaction mixture in nitrogen. The reaction mixture was heated to 110 °C, and then two drops of acetic acid were added. The resulting mixture was refluxed for 4 h. After the reaction was completed, the toluene was removed under reduced pressure. The residue was purified by silica gel column chromatography using DCM/hexane (1/5, v/v) as eluent to give compound **3a** as a green solid (102 mg, 78%). ¹H NMR (400 MHz, CDCl₃): δ 7.65–7.61 (m, 6H), 7.29 (s, *J*=8.0 Hz, 2H), 6.96 (q, *J*=8.0 Hz, 4H), 6.70 (d, *J*=8.0 Hz, 2H), 3.88 (s, 6H), 1.73 (s, 6H). ¹³C NMR (100 MHz, CDCl₃): 160.8, 160.6, 154.1, 139.7, 137.3, 136.6, 132.8, 129.4, 129.3, 129.2, 118.4, 118.0, 116.9, 114.4, 114.3, 55.4, 51.8. ¹⁹F NMR (376 MHz, CDCl₃): δ -159.78 (m, 2F), -150.84 (t, 1F), -142.20 (q, 2F), -138.75 (q, 2F). HRMS (ESI): [M]⁺=650.1922; calcd for C₃₅H₂₆BF₇N₂O₂: 650.1947.

4.2.5. Synthesis of 3,5-bis(9*H*-carbazol-3-vinyl)-8-pentafluorophenyl-4,4-difluoro-4-borata-3a,4a-diaza-*s*-indacene (3b**).** Compound **2** (82 mg, 0.2 mmol) and 6-(3-formyl-9*H*-carbazol-9-yl)hexyl acetate (148 mg, 0.44 mmol) were dissolved in 25 mL of toluene in a three-neck round bottom flask. Two drops of

piperidine were added to the reaction mixture in nitrogen. The reaction mixture was heated to 110 °C, and then two drops of acetic acid were added. The resulting mixture was refluxed for 4 h. After the reaction was completed, the toluene was removed under reduced pressure. The residue was purified by silica gel column chromatography using DCM/hexane (1/3, v/v) as eluent to give compound **3b** as a green solid (172 mg, 82%). ¹H NMR (400 MHz, CDCl₃): δ 8.23 (d, *J*=8 Hz, 2H), 7.85 (t, *J*=8 Hz, 4H), 7.53 (t, *J*=8 Hz, 4H), 7.42 (m, 4H), 7.32 (t, *J*=8 Hz, 4H), 6.76 (s, 2H), 4.31 (t, *J*=6.8 Hz, 4H), 4.04 (t, *J*=6.8 Hz, 4H), 3.35 (s, 4H), 2.04 (s, 6H), 1.91 (t, *J*=6.8 Hz, 4H), 1.24 (m, 14H). ¹³C NMR (100 MHz, CDCl₃): 171.2, 153.8, 141.2, 140.9, 139.9, 138.4, 133.4, 127.9, 126.1, 125.8, 123.4, 122.9, 120.7, 120.4, 119.9, 119.5, 118.2, 116.4, 109.1, 109.0, 64.4, 52.5, 43.1, 28.9, 28.5, 26.9, 26.4, 25.8, 24.0, 21.0. ¹⁹F NMR (376 MHz, CDCl₃) δ -159.82 (m, 2F), -150.90 (t, 1F), -142.22 (q, 2F), -138.98 (q, 2F). HRMS (ESI): [M]⁺=1052.4257; calcd for C₆₁H₅₆BF₇N₄O₄: 1052.4284.

4.3. UV–vis–NIR absorption and emission spectra measurements

UV–vis spectra were recorded on a Hitachi UV-3310 spectrometer. Fluorescence spectra were recorded on a Hitachi FL-4500 fluorometer. Mass spectra were measured on a HP-1100 LC–MS spectrometer. The ¹H NMR and ¹³C NMR spectra were recorded on a Bruker AV-400 spectrometer with tetramethylsilane (TMS) as the internal standard. The chemical shift was recorded in parts per million and the following abbreviations were used to explain the multiplicities: s=singlet, d=doublet, t=triplet, m=multiplet, br=broad.

4.4. Computation details

The ground state geometries were optimized by employing the hybrid B3LYP⁴³ function and a 6–31G** basis set. Vertical excitation energies were calculated by time-dependent density functional theory (TD-DFT) at MPW1K⁴⁴/6–31G** and levels of theory. All calculations were carried out with Gaussian 09 program packages.⁴⁵

4.5. Confocal fluorescence imaging

HeLa cells were cultured in RPMI 1640 medium (Invitrogen) containing 10% fetal bovine serum, penicillin (100 units/mL), streptomycin (100 µg/mL), and 5% CO₂ at 37 °C. One day before experiment, cell suspensions were plated at a density of 1.0×10⁴ cells/mL on 35 mm diameter round glass coverslips. Then, the cells were incubated with **1b** (10 µM) for 1 h at 37 °C in 5% CO₂–95% air and washed three times with PBS buffer (0.10 M, pH 7.40) before imaging. Fluorescent images were acquired on a Nikon A1 confocal laser-scanning microscope with a 60× objective lens.

Acknowledgements

We acknowledge the financial support from NSFC (No. 21203138, 21103123, 31371750), the Natural Science Foundation of Tianjin (13JCQNJC05300), Hubei Provincial Educational Department (D20132702), and National Innovation Training Program of Undergraduates (No. 201310060025).

Supplementary data

Supplementary data related to this article can be found at <http://dx.doi.org/10.1016/j.tet.2014.06.040>.

References and notes

- Loudet, A.; Burgess, K. *Chem. Rev.* **2007**, *107*, 4891–4932.
- Ulrich, G.; Ziesse, R.; Harriman, A. *Angew. Chem., Int. Ed.* **2008**, *47*, 1184–1201.
- Boens, N.; Leen, V.; Dehaen, W. *Chem. Soc. Rev.* **2012**, *41*, 1130–1172.
- Piatkevich, K. D.; Subach, F. V.; Verkhusha, V. V. *Chem. Soc. Rev.* **2013**, *42*, 3441–3452.
- Knaus, H. G.; Moshhammer, T.; Friedrich, K.; Kang, H. C.; Haugland, R. P.; Glossmann, H. *Proc. Natl. Acad. Sci. U.S.A.* **1992**, *89*, 3586–3590.
- Merino, E. J.; Weeks, K. M. *J. Am. Chem. Soc.* **2005**, *127*, 12766–12767.
- Peters, C.; Billich, A.; Ghobrial, M.; Hoegenauer, K.; Ullrich, T.; Nussbaumer, P. *J. Org. Chem.* **2007**, *72*, 1842–1845.
- Yamada, K.; Nomura, Y.; Citterio, D.; Iwasawa, N.; Suzuki, K. *J. Am. Chem. Soc.* **2005**, *127*, 6956–6957.
- Hudnall, T. W.; Gabbai, F. P. *Chem. Commun.* **2008**, 4596–4597.
- Domaille, D. W.; Zeng, L.; Chang, C. J. *J. Am. Chem. Soc.* **2010**, *132*, 1194–1195.
- Atilgan, S.; Ozdemir, E.; Akkaya, E. U. *Org. Lett.* **2010**, *12*, 4792–4795.
- Gorman, A.; Killoran, J.; O'Shea, C.; Kenna, T.; Gallagher, W. M.; O'Shea, D. F. *J. Am. Chem. Soc.* **2004**, *126*, 10619–10631.
- Atilgan, S.; Ekmekci, Z.; Dogan, A. L.; Guc, D.; Akkaya, E. U. *Chem. Commun.* **2006**, 4398–4400.
- Hattori, S. K.; Ohkubo, K.; Urano, Y.; Sunahara, H.; Nagano, T.; Wada, Y.; Tkachenko, N. V.; Lemmetyinen, H.; Fukuzumi, S. *J. Phys. Chem. B* **2005**, *109*, 15368–15375.
- Erten-Ela, S.; Yilmaz, M. D.; Icli, B.; Dede, Y.; Icli, S.; Akkaya, E. U. *Org. Lett.* **2008**, *10*, 3299–3302.
- Rousseau, T.; Cravino, A.; Bura, T.; Ulrich, G.; Ziesse, R.; Roncali, J. *Chem. Commun.* **2009**, 1673–1675.
- Lai, R. Y.; Bard, A. J. *J. Phys. Chem. B* **2003**, *107*, 5036–5042.
- Hepp, A.; Ulrich, G.; Schmechel, R.; von Seggern, H.; Ziesse, R. *Synth. Met.* **2004**, *146*, 11–15.
- Bonardi, L. K.; Camerel, F.; Jolinat, P.; Retailleau, P.; Ziesse, R. *Adv. Funct. Mater.* **2008**, *18*, 401–413.
- Ntziachristos, V.; Tung, C. H.; Bremer, C.; Weissleder, R. *Nat. Med.* **2002**, *8*, 757–760.
- Yuan, L.; Lin, W. Y.; Zheng, K.; He, L.; Huang, W. *Chem. Soc. Rev.* **2013**, *42*, 622–661.
- Killoran, J.; Allen, L.; Gallagher, J. F.; Gallagher, W. M.; O'Shea, D. F. *Chem. Commun.* **2002**, 1862–1863.
- Shen, Z.; Röhr, H.; Rurack, K.; Uno, H.; Spieles, M.; Schulz, B.; Reck, G.; Ono, N. *Chem.—Eur. J.* **2004**, *10*, 4853–4871.
- Jiao, L. J.; Yu, C. J.; Liu, M. M.; Wu, Y. C.; Cong, K. B.; Meng, T.; Wang, Y.; Hao, E. *J. Org. Chem.* **2010**, *75*, 6035–6038.
- Baruah, M.; Qin, W. W.; VallQe, R. A. L.; Beljonne, D.; Rohand, T.; Dehaen, W.; Boens, N. *Org. Lett.* **2005**, *7*, 4377–4380.
- Yu, Y. H.; Descalzo, A. B.; Shen, Z.; Röhr, H.; Liu, Q.; Wang, Y. W.; Spieles, M.; Li, Y. Z.; Rurack, K.; You, X. Z. *Chem.—Asian J.* **2006**, *1*, 176–187.
- Deniz, E.; Isbasar, C. C.; Bozdemir, A.; Yildirim, L. T.; Siemiarczuk, A.; Akkaya, E. U. *Org. Lett.* **2008**, *10*, 3401–3404.
- Buyukcakar, O.; Bozdemir, O. A.; Kolemen, S.; Erbas, S.; Akkaya, E. U. *Org. Lett.* **2009**, *11*, 4644–4647.
- Zhao, W.; Carreira, E. M. *Angew. Chem., Int. Ed.* **2005**, *44*, 1677–1679.
- Zhao, W.; Carreira, E. M. *Chem.—Eur. J.* **2006**, *12*, 7254–7263.
- McDonnell, S. O.; O'Shea, D. F. *Org. Lett.* **2006**, *8*, 3493–3496.
- Zhang, D. K.; Martin, V.; Moreno, I. G.; Costela, A.; Ojeda, M. E. P.; Xiao, Y. *Phys. Chem. Chem. Phys.* **2011**, *13*, 13026–13033.
- Rurack, K.; Kollmannsberger, M.; Daub, J. *Angew. Chem., Int. Ed.* **2001**, *40*, 385–387.
- Rurack, K.; Kollmannsberger, M.; Daub, J. *New J. Chem.* **2001**, *25*, 289–292.
- Coskun, A.; Akkaya, E. U. *Tetrahedron Lett.* **2004**, *45*, 4947–4949.
- Dost, Z.; Atilgan, S.; Akkaya, E. U. *Tetrahedron* **2006**, *62*, 8484–8488.
- Gibbs, J. H.; Robins, L. T.; Zhou, Z. H.; Bobadova-Parvanova, P.; Cottam, M.; McCandless, G. T.; Fronczek, F. R.; Vicente, M. G. H. *Bioorg. Med. Chem.* **2013**, *21*, 5770–5781.
- Kubin, R. F.; Fletcher, A. N. *J. Lumin.* **1983**, *27*, 455–462.
- Chen, Y. H.; Zhao, J. Z.; Guo, H. M.; Xie, L. J. *J. Org. Chem.* **2012**, *77*, 2192–2206.
- Lee, M. H.; Yoon, B.; Kim, J. S.; Sessler, J. L. *Chem. Sci.* **2013**, *4*, 4121–4126.
- Liu, H.; Wang, Y.; Liu, C.; Li, H.; Gao, B.; Zhang, L.; Bo, F.; Bai, Q.; Ba, X. *J. Mater. Chem.* **2012**, *22*, 6176–6181.
- Jiao, C. J.; Huang, K. W.; Wu, J. S. *Org. Lett.* **2011**, *13*, 632–635.
- Becke, A. D. *J. Chem. Phys.* **1993**, *98*, 1372–1377.
- Lynch, B. J.; Fast, P. L.; Harris, M.; Truhlar, D. G. *J. Phys. Chem. A* **2000**, *104*, 4811–4815.
- Frisch, M. J.; Trucks, G. W.; Schlegel, H. B.; Scuseria, G. E.; Robb, M. A.; Cheeseman, J. R.; Scalmani, G.; Barone, V.; Mennucci, B.; Petersson, G. A.; Nakatsuji, H.; Caricato, M.; Li, X.; Hratchian, H. P.; Izmaylov, A. F.; Bloino, J.; Zheng, G.; Sonnenberg, J. L.; Hada, M.; Ehara, M.; Toyota, K.; Fukuda, R.; Hasegawa, J.; Ishida, M.; Nakajima, T.; Honda, Y.; Kitao, O.; Nakai, H.; Vreven, T.; Montgomery, J. A.; Peralta, J. E.; Ogliaro, F.; Bearpark, M.; Heyd, J. J.; Brothers, E.; Kudin, K. N.; Staroverov, V. N.; Kobayashi, R.; Normand, J.; Raghavachari, K.; Rendell, N.; Burant, J. C.; Iyengar, S. S.; Tomasi, J.; Cossi, M.; Rega, N.; Millam, J. M.; Klene, N.; Knox, J. E.; Cross, J. B.; Bakken, V.; Adamo, C.; Jaramillo, J.; Gomperts, R.; Stratmann, R. E.; Yazyev, O.; Austin, A. J.; Cammi, R.; Pomelli, C.; Ochterski, J. W.; Martin, R. L.; Morokuma, K.; Zakrzewski, V. G.; Voth, G. A.; Salvador, P.; Dannenberg, J. J.; Dapprich, S.; Daniels, A. D.; Farkas, O.; Foresman, J. B.; Ortiz, J. B.; Cioslowski, J.; Fox, D. J. *Gaussian 09, Revision A.1*; Gaussian: Wallingford, CT, 2009.